Application of the Implicit MacCormack Scheme to the Parabolized Navier-Stokes Equations

Scott L. Lawrence* and J. C. Tannehill†
Iowa State University, Ames, Iowa
and
Denny S. Chaussee‡
NASA Ames Research Center, Moffett Field, California

MacCormack's implicit finite difference scheme has been used to solve the two-dimensional, parabolized Navier-Stokes (PNS) equations. This method for solving the PNS equations does not require the inversion of block tridiagonal systems of algebraic equations and permits the original explicit MacCormack scheme to be employed in those regions where implicit treatment is not needed. The advantages and disadvantages of the present adaptation are discussed in relation to those of the conventional Beam-Warming scheme for a flat-plate boundary-layer test case. Comparisons are made for accuracy, stability, computer time, computer storage, and ease of implementation. The present method is also applied to a second test case of hypersonic laminar flow over a 15 deg compression corner. The computed results compare favorably with experiment and a numerical solution of the complete Navier-Stokes equations.

Introduction

NUMEROUS studies in recent years have demonstrated the usefulness of parabolized Navier-Stokes (PNS) equations in the calculation of a definable class of supersonic flows. If the inviscid region of the flow is supersonic and there is no streamwise separation of the flow, the equations of motion can be accurately modeled by a mixed set of hyperbolic-parabolic equations (the PNS equations). These equations can be solved much more efficiently than the complete Navier-Stokes equations since the solution can be marched in space rather than time.

The PNS equations have been integrated using a variety of finite difference schemes. Currently, noniterative, implicit, approximate-factorization schemes developed by Vigneron et al. and Schiff and Steger[2] are frequently used. These schemes are based on a class of alternating direction implicit (ADI) schemes developed by Lindemuth and Killeen,[3] Briley and McDonald,[4] and Beam and Warming,[5] and require the inversion of block tridiagonal systems of algebraic equations in the calculation of flow properties at each marching step.

MacCormack[6] has devised an implicit scheme that requires only the inversion of block bidiagonal systems rather than block tridiagonal systems, thus yielding a savings in computer time and storage requirements. This scheme was designed to solve time-dependent equations such as the complete Navier-Stokes equations. It is based on MacCormack's well-proven second-order accurate explicit predictor-corrector method[7] but adds an implicit procedure in the predictor-corrector sequence for points in the flow at which the local CFL number exceeds the stability limit. The method has been applied to two-dimensional internal supersonic flows,[8,9] two-dimensional external flows,[10] external axisymmetric flows,[11] quasi-one-dimensional flows,[12] three-dimensional flows over a biconic with a compression flap,[13] as well as three-dimensional blunt-body flows. Except for the case of Ref. 11, the scheme was applied to either the complete or thin layer forms of the unsteady Navier-Stokes equations. In Ref. 11, the scheme was applied to the viscous shock-layer equations.

In the present work, the implicit MacCormack scheme has been modified to solve the PNS equations. This paper describes the resulting finite difference algorithm and presents computational results for two laminar test cases. Results for the case of a flat-plate boundary layer are compared with those obtained from a boundary-layer code. In a more severe test of the method, the hypersonic flow past a 15 deg compression corner has been computed. For this case, a global iteration on the pressure field of the form developed by Rakich[14] was applied. Using an iteration of this type, it is possible to include influences from downstream that are otherwise neglected in a PNS calculation. The computed results are compared with available experimental data and a numerical solution of the complete Navier-Stokes equations.

Governing Equations

The equations describing the planar flow of a Newtonian fluid are the two-dimensional, unsteady Navier-Stokes equations. These can be written in nondimensional strong-conservation-law form in Cartesian coordinate as

$$\frac{\partial U}{\partial t}+\frac{\partial (E-E_v)}{\partial x}+\frac{\partial (F-F_v)}{\partial y}=0 \tag{1}$$

where

$$U=[\rho,\ \rho u,\ \rho v,\ e_t]^T$$

$$E=[\rho u,\ \rho u^2+p,\ \rho uv,\ (e_t+p)u]^T$$

$$F=[\rho v,\ \rho uv,\ \rho v^2+p,\ (e_t+p)v]^T$$

$$E_v=[0,\ \tau_{xx},\ \tau_{xy},\ u\tau_{xx}+v\tau_{xy}-q_x]^T$$

$$F_v=[0,\ \tau_{xy},\ \tau_{yy},\ u\tau_{xy}+v\tau_{yy}-q_y]^T$$

Presented as Paper 83-1956 at the AIAA 6th Computational Fluid Dynamics Conference, Danvers, Mass., July 13-15, 1983; received July 22, 1983; revision received Feb. 9, 1984.

*Research Assistant, Department of Aerospace Engineering and Computational Fluid Dynamics Institute.
†Professor, Department of Aerospace Engineering and Computational Fluid Dynamics Institute. Associate Fellow AIAA.
‡Research Scientist. Member AIAA.

and

$$\tau_{xx}=\frac{\mu}{Re_\infty}\frac{2}{3}\left(2\frac{\partial u}{\partial x}-\frac{\partial v}{\partial y}\right), \qquad \tau_{yy}=\frac{\mu}{Re_\infty}\frac{2}{3}\left(-\frac{\partial u}{\partial x}+2\frac{\partial v}{\partial y}\right)$$

$$\tau_{xy}=\frac{\mu}{Re_\infty}\left(\frac{\partial u}{\partial y}+\frac{\partial v}{\partial x}\right)$$

$$q_x=-\frac{\mu}{Re_\infty}\frac{1}{(\gamma-1)M_\infty^2 Pr}\frac{\partial T}{\partial x}, \quad q_y=-\frac{\mu}{Re_\infty}\frac{1}{(\gamma-1)M_\infty^2 Pr}\frac{\partial T}{\partial y}$$

$$e_t=\rho\left(e+\frac{u^2+v^2}{2}\right)$$

The equations have been nondimensionalized (dimensional quantities are denoted by a tilde) in the following manner:

$$t=\tilde{t}/(\tilde{L}/\tilde{V}_\infty) \qquad x=\tilde{x}/\tilde{L} \qquad y=\tilde{y}/\tilde{L}$$

$$u=\tilde{u}/\tilde{V}_\infty \qquad v=\tilde{v}/\tilde{V}_\infty \qquad e=\tilde{e}/\tilde{V}_\infty^2$$

$$\rho=\tilde{\rho}/\tilde{\rho}_\infty, \quad T=\tilde{T}/\tilde{T}_\infty, \quad \mu=\tilde{\mu}/\tilde{\mu}_\infty, \quad p=\tilde{p}/\tilde{\rho}_\infty\tilde{V}_\infty^2$$

where $\tilde{L}$ is the reference length of unity.

The Reynolds number (Re_∞) appearing in the viscous terms is given by

$$Re_\infty=\tilde{\rho}_\infty\tilde{V}_\infty\tilde{L}/\tilde{\mu}_\infty$$

The coefficient of thermal conductivity has been replaced by assuming a constant Prandtl number and the coefficient of viscosity is calculated using Sutherland's equation

$$\mu=T^{3/2}\left(\frac{1+110.4K/\tilde{T}_\infty}{T+110.4K/\tilde{T}_\infty}\right)$$

Finally, the system is closed using the perfect gas equation of state, which in nondimensional form becomes

$$p=\rho T/\gamma M_\infty^2$$

Coordinate Transformation

A transformation of the spatial coordinates of the form

$$\xi=x, \quad \eta=\eta(x,y)$$

is applied to Eq. (1) so that the equation may be differenced on a uniform computational mesh. The resulting equation in strong-conservation-law form is

$$\frac{\partial\hat{U}}{\partial t}+\frac{\partial\hat{E}}{\partial\xi}+\frac{\partial\hat{F}}{\partial\eta}=0 \tag{2}$$

where

$$\hat{U}=\frac{U}{J}, \quad \hat{E}=\frac{1}{J}(E-E_v)$$

$$\hat{F}=\frac{1}{J}[\eta_x(E-E_v)+\eta_y(F-F_v)]$$

and J is the Jacobian of the transformation given by

$$J=\frac{\partial(\xi,\eta)}{\partial(x,y)}$$

Derivatives of the viscous vectors are transformed using the chain rule.

Parabolizing Assumptions

The equations are "parabolized" to permit stable marching in space by making the following assumptions:

1) The flow is steady.

2) Streamwise viscous derivatives are negligible in comparison with normal viscous derivatives. This approximation is valid for flows with high Reynolds numbers.

The following system of PNS equations is obtained as a result of these assumptions:

$$\frac{\partial\bar{E}}{\partial\xi}+\frac{\partial\bar{F}}{\partial\eta}=0 \tag{3}$$

where

$$\bar{E}=\frac{1}{J}E, \quad \bar{F}=\frac{1}{J}[\eta_x(E-E_v)+\eta_y(F-F_v)]$$

and E_v and F_v now contain no ξ derivative terms. The PNS equations are a mixed set of hyperbolic-parabolic equations in the streamwise direction ξ provided that the inviscid flow is supersonic, the streamwise velocity component is everywhere greater than zero, and the streamwise pressure gradient term in the streamwise momentum equation is either omitted or the "departure behavior" is suppressed by a suitable technique.

Streamwise Pressure Gradient

The presence of the streamwise pressure gradient term in the streamwise momentum equation permits information to be propagated upstream through subsonic portions of the flowfield such as the boundary layer. As a consequence, a space-marching method of solution is not well-posed and in some cases exponentially growing solutions (departure solutions) are encountered. A number of different techniques have been proposed to eliminate this difficulty. For this study, the method proposed by Vigneron et al.[1] is used.

The "Vigneron technique" involves splitting the $\bar{E}$ vector into two parts,

$$\bar{E}=\bar{E}^*+\bar{P}$$

where

$$\bar{E}^*=\frac{1}{J}[\rho u, \ \rho u^2+\omega p, \ \rho uv, \ (e_t+p)u]^T$$

$$\bar{P}=\frac{1}{J}[0, \ (1-\omega)p, \ 0, \ 0]^T$$

The $\bar{E}^*$ vector now replaces $\bar{E}$ in the numerical scheme and $\bar{P}_\xi$ is treated as a source term that is evaluated in the supersonic region. The final form of the governing equations becomes

$$\frac{\partial\bar{E}^*}{\partial\xi}+\frac{\partial\bar{F}}{\partial\eta}+\frac{\partial\bar{P}}{\partial\xi}=0 \tag{4}$$

An eigenvalue analysis shows that this system will be hyperbolic-parabolic if

$$\omega<\frac{\gamma M_\xi^2}{1+(\gamma-1)M_\xi^2}$$

where M_ξ is the local streamwise Mach number. Since this relation was determined using a linear analysis, a safety factor is applied and ω is calculated from the resulting expression or is set equal to one when the computed ω is greater than one.

Numerical Solution of Equations

Numerical Scheme

The numerical scheme used in the present study to integrate the PNS equations is an adaptation of the method proposed

by MacCormack[6] in 1981. MacCormack demonstrated the method's usefulness for solving the full unsteady Navier-Stokes equations in an application to a two-dimensional shock/boundary-layer interaction problem. The method is implicit in nature and thus allows a much larger marching step size than explicit methods. In addition, the method possesses three advantages over conventional fully implicit methods. First, the method uses two-point, one-sided differences in the implicit part of the algorithm. Thus, block bidiagonal systems of algebraic equations result that are less costly to invert than the block tridiagonal systems found in conventional methods. Second, the method employs the inviscid Jacobians and corrects them using representative viscous terms added to the Eulerian eigenvalues. This maintains stability while avoiding the expensive calculation of the complete viscous Jacobians. Finally, the algorithm allows the implicit step to be skipped in regions where the explicit stability restriction is satisfied, as in the region away from the boundary layer where mesh spacing is large. The method is stable for unbounded Δt and second-order accurate under the condition that $(\mu/\rho)[\Delta t/\min(\Delta x^2, \Delta t^2)]$ remains bounded as a two-dimensional Cartesian mesh is refined.

In adapting this scheme for use in solving Eq. (4), the procedure outlined in Ref. 6 is followed. Equation (4) is differentiated with respect to ξ to obtain the equation

$$\frac{\partial}{\partial \xi}\left(\frac{\partial \bar{E}^*}{\partial \xi}\right)+\frac{\partial}{\partial \eta}\left(C\frac{\partial \bar{E}^*}{\partial \xi}\right)+\frac{\partial^2 \bar{P}}{\partial \xi^2}=0 \tag{5}$$

which governs the propagation of the local changes, $\Delta\xi \times (\partial \bar{E}^*/\partial \xi)$. In Eq. (5), C is the Jacobian $\partial \bar{F}/\partial \bar{E}^*$. If the ξ derivative is implicitly differenced, the following equation results:

$$\left(I+\Delta\xi\frac{\partial C\cdot}{\partial \eta}\right)\left(\frac{\partial \bar{E}^*}{\partial \xi}\right)^{n+1}=\left(\frac{\partial \bar{E}}{\partial \xi}\right)^{n}-\left(\frac{\partial \bar{P}}{\partial \xi}\right)^{n+1} \tag{6}$$

where the dot indicates that the derivative also operates on the factor to the right. Next, define

$$\Delta \bar{E}^n=\Delta\xi\left(\frac{\partial \bar{E}}{\partial \xi}\right)^n \quad \text{and} \quad \delta \bar{E}^{*n+1}=\Delta\xi\left(\frac{\partial \bar{E}^*}{\partial \xi}\right)^{n+1}$$

so that Eq. (6) becomes

$$\left(I+\Delta\xi\frac{\partial C\cdot}{\partial n}\right)\delta \bar{E}^{*n+1}=\Delta \bar{E}^n-\Delta \bar{P}^{n+1} \tag{7}$$

At this point, it is observed that proceeding to difference this equation in the same manner that MacCormack used for the unsteady equations will yield a scheme that requires the modal analysis (i.e., finding the eigenvalues and eigenvectors) of the C matrix. In addition, the difficult task of decoding the $\bar{E}^*$ vector will be encountered at each step in order to obtain the flow variables.

The decoding problem consists of solving the nonlinear set of algebraic equations

$$\begin{bmatrix} \rho u \\ \rho u^2+\omega p \\ \rho u v \\ (e_t+p)u \end{bmatrix} = J\bar{E}^* \tag{8}$$

for the dependent variables ρ, u, v, and p. This system can be reduced to a single quadratic equation for u velocity, with one root of this equation being associated with a supersonic flow and the other with a subsonic flow. Solution is straightforward when it is known a priori that the flow is supersonic everywhere, as when integrating the Euler equations. However, for viscous problems, the solution is more difficult due to the presence of the subsonic region of the boundary layer.

In order to avoid this problem, as well as the modal analysis of the C matrix, Eq. (7) is modified using the linearization

$$(\delta \bar{E}^*)^{n+1}=\Delta\xi\left(\frac{\partial \bar{E}^*}{\partial \bar{U}}\right)^n\left(\frac{\partial \bar{U}}{\partial \xi}\right)^{n+1}+O(\Delta\xi)^2$$

or

$$\delta \bar{E}^{*n+1}=A^n\delta \bar{U}^{n+1}+O(\Delta\xi)^2 \tag{9}$$

where

$$A=\frac{\partial \bar{E}^*}{\partial \bar{U}}$$

and

$$\delta \bar{U}^{n+1}=\Delta\xi\left(\frac{\partial \bar{U}}{\partial \xi}\right)^{n+1}$$

Finally, noting that

$$\frac{\partial \bar{F}}{\partial \bar{E}^*}=\left(\frac{\partial \bar{F}}{\partial \bar{U}}\right)\left(\frac{\partial \bar{E}^*}{\partial \bar{U}}\right)^{-1}$$

and substituting Eq. (9) into Eq. (7), we have

$$\left(A+\Delta\xi\frac{\partial B}{\partial \eta}\cdot\right)\delta \bar{U}^{n+1}=\Delta \bar{E}^n-\Delta \bar{P}^{n+1} \tag{10}$$

where

$$B=\frac{\partial \bar{F}}{\partial \bar{U}}$$

The equation now contains the simpler Jacobians, A and B, and the easily decoded $\bar{U}$ vector. Additional justification for this change in the dependent variable is provided by consideration of the case of a more general transformation of the streamwise coordinate. For example, a transformation of the form $\xi=\xi(x,y)$ allows the marching planes to be of general shape and orientation, which is desirable for marching along bodies with large surface slopes. However, this transformation also yields an $\bar{E}^*$ vector that is virtually impossible to decode, thus making a change in the marching vector from $\bar{E}^*$ to $\bar{U}$ essential. The disadvantages of the present formulation will be discussed in a subsequent paragraph.

Differencing Eq. (10) in a manner consistent with MacCormack's original explicit scheme[7] yields the following implicit predictor-corrector algorithm for the numerical integration of Eq. (4):

Predictor,

$$\Delta \bar{E}_j^n=-\Delta\xi\frac{\Delta_+ \bar{F}_j^n}{\Delta\eta} \tag{11a}$$

$$\left(A_j^n-\Delta\xi\frac{\Delta_+}{\Delta\eta}|B|\cdot\right)\delta \bar{U}_j^{\overline{n+1}}=\Delta \bar{E}_j^n-\Delta \bar{P}_j^n \tag{11b}$$

$$\bar{U}_j^{\overline{n+1}}=\bar{U}_j^n+\delta \bar{U}_j^{\overline{n+1}} \tag{11c}$$

Corrector,

$$\Delta \bar{E}_j^{\overline{n+1}}=-\Delta\xi\frac{\Delta_- \bar{F}_j^{\overline{n+1}}}{\Delta\eta} \tag{12a}$$

$$\left(A_j^{\overline{n+1}}+\Delta\xi\frac{\Delta_-}{\Delta\eta}|B|\cdot\right)\delta \bar{U}_j^{n+1}=\Delta \bar{E}_j^{\overline{n+1}}-\Delta \bar{P}_j^n \tag{12b}$$

$$\bar{U}_j^{n+1}=\tfrac{1}{2}(\bar{U}_j^n+\bar{U}_j^{\overline{n+1}}+\delta \bar{U}_j^{n+1}) \tag{12c}$$

The differencing operators, $\Delta_+/\Delta\eta$ and $\Delta_-/\Delta\eta$ are defined by

$$\frac{\Delta_+ z}{\Delta\eta}=\frac{z_{j+1}-z_j}{\Delta\eta}, \quad \frac{\Delta_- z}{\Delta\eta}=\frac{z_j-z_{j-1}}{\Delta\eta}$$

The right-hand sides of Eqs. (11a) and (12a) are calculated as in the explicit scheme. That is, one-sided differences are used for the convective terms and central differences for the viscous terms. In the present code, the differencing permutation can be reversed at each marching step except when using the implicit wall boundary condition procedure described below.

The matrix B in Eq. (10) has been replaced with the related matrix $|B|$ in the implicit steps of the algorithm. This substitution is required in order for the block bidiagonal systems to be inverted numerically in a stable manner. The matrix $|B|$ is defined by

$$|B|=S_y^{-1}D_B S_y \tag{13}$$

where S_y is the matrix whose rows are the left eigenvectors of the inviscid Jacobian, $B_i=\partial\bar{F}_i/\partial\bar{U}$ (see the Appendix). D_B is the diagonal matrix whose elements d_{B_i} are defined by

$$d_{B_i}=K(\,|\lambda_i|+\text{VISCOR})$$

where λ_i is the ith eigenvalue of B_i (see Appendix A). The viscous correction, VISCOR, is related to the eigenvalues of the viscous Jacobian $\partial\bar{F}_v/\partial\bar{U}$ and is given by

$$\text{VISCOR}=\frac{2\mu}{Re_\infty}\frac{\eta_x^2+\eta_y^2}{\rho\Delta\eta}$$

The coefficient K is determined by

$$K=\max\left[1.-\frac{\sigma(\Delta\xi)_{\text{CFL}}}{\Delta\xi\,[1+(2/Re_\Delta)]}, \quad 0\right]$$

where

$$Re_\Delta=\frac{\rho u\Delta\eta}{\mu\eta_y}Re_\infty$$

and σ is a safety factor usually set equal to 0.5. Also, $(\Delta\xi)_{\text{CFL}}$ is the largest step size satisfying the CFL condition

$$(\Delta\xi)_{\text{CFL}}\le\Delta\eta/\lambda_c$$

where λ_c is the maximum eigenvalue of $\partial\bar{F}_i/\partial\bar{E}^*$. Thus, when the step size is such that the explicit scheme is locally stable, K is set to zero and the implicit step reduces to

$$[A_j]\delta\bar{U}_j=\Delta\bar{E}_j-\Delta\bar{P}_j \tag{14}$$

This matrix equation reveals a disadvantage of marching with the $\bar{U}$ vector inasmuch as it is necessary to invert a 4×4 matrix at each point, including those at which the explicit scheme is stable. The other drawback of this formulation is that the main diagonal blocks of the resulting coefficient matrices cannot be easily diagonalized as MacCormack has done. A lower-upper decomposition is used here to invert the main diagonal blocks. It is believed, however, that the computer time saved by diagonalizing the coefficient matrices would be spent in decoding the $\bar{E}^*$ vector. In order to remedy the first disadvantage, steps b and c of Eqs. (11) and (12) may be replaced with

Predictor,

$$\bar{E}^{*\overline{n+1}}_j=\bar{E}^{*n}_j+\Delta\bar{E}^n_j-\Delta\bar{P}^n_j \tag{15}$$

Corrector,

$$\bar{E}^{*n+1}_j=\tfrac{1}{2}(\bar{E}^{*n}_j+\bar{E}^{*\overline{n+1}}_j++\Delta\bar{E}^{\overline{n+1}}_j-\Delta\bar{P}^n)$$

in regions of the flow where the flow properties and grid spacing are such that the marching step size satisfies the stability restriction of the explicit scheme. Generally, the explicit scheme will not be stable in the subsonic region of the boundary layer, so that decoding is not a problem unless a more general transformation has been applied.

The implicit smoothing proposed by MacCormack was found to be unnecessary for the test cases of the present study. However, when capturing shocks some explicit damping is required. The pressure smoothing term of Ref. 15 was found to be sufficient to allow stable space marching. This scheme involves adding a term proportional to the quantity $(\Delta\eta)^4\,|P_{\eta\eta}|\,U_{\eta\eta}$ so that the smoothing effect is most pronounced in regions of high pressure gradient changes. In the present code, the term is centrally differenced as

$$\bar{E}^*_j=C_x\frac{|p_{j+1}-2p_j+p_{j-1}|}{p_{j+1}+2p_j+p_{j-1}}\frac{(U_{j+1}-2U_j+U_{j-1})}{J_j}$$

where C_x is proportional to the marching step size. This term is fourth order in $\Delta\eta$ so that little effect on the viscous forces is observed.

Computational Grid

For viscous flow cases, it is desirable to obtain as much resolution of the boundary layer as possible in order that the viscous stresses may be accurately modeled. This is accomplished in the present study by clustering the grid points normal to the wall using the following clustering function:

$$z(\eta)=\frac{\beta+1-(\beta-1)\,[(\beta+1)/(\beta-1)]^{1-\eta}}{[(\beta+1)/(\beta-1)]^{1-\eta}+1}$$

where $z(\eta)$ becomes equal to one when $\eta=1$ and is zero when $\eta=0$. The points become more tightly clustered as β approaches 1.

The physical distance y is then obtained from

$$y(\xi,\eta)=y_0(\xi)+\delta(\xi)z(\eta)$$

where $\delta(\xi)$ is the distance from the wall to the freestream edge of the grid and $y_0(\xi)$ the value of y at the wall.

The transformation used is analytic and the metrics could therefore be determined analytically. However, experience has shown that it is desirable to calculate the terms η_x and η_y numerically in a manner consistent with the finite difference scheme being used. For the MacCormack scheme, one-sided differences are used to evaluate the Jacobian of the transformation J. The differencing follows that of the convective derivatives. The Jacobian can be calculated by the equation

$$J=1/y_\eta$$

The metrics are then computed using the relations

$$\eta_x=-Jy_\xi, \quad \eta_y=J$$

and

$$y_\xi(\eta)=y_{0_\xi}(\xi)+\delta_\xi(\xi)z(\eta)$$

Boundary Conditions

At the wall boundary, no-slip conditions were imposed on the velocities and the temperature was specified. In order to determine the wall pressure, a zero-gradient extrapolation was explicitly applied to the pressure at the end of each predictor and corrector sweep. At the freestream edge of the grid, zero-gradient extrapolations were explicitly applied to all of the

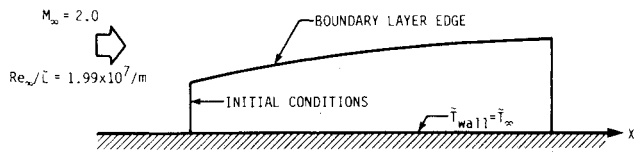

Fig. 1 Flat-plate boundary-layer test case.

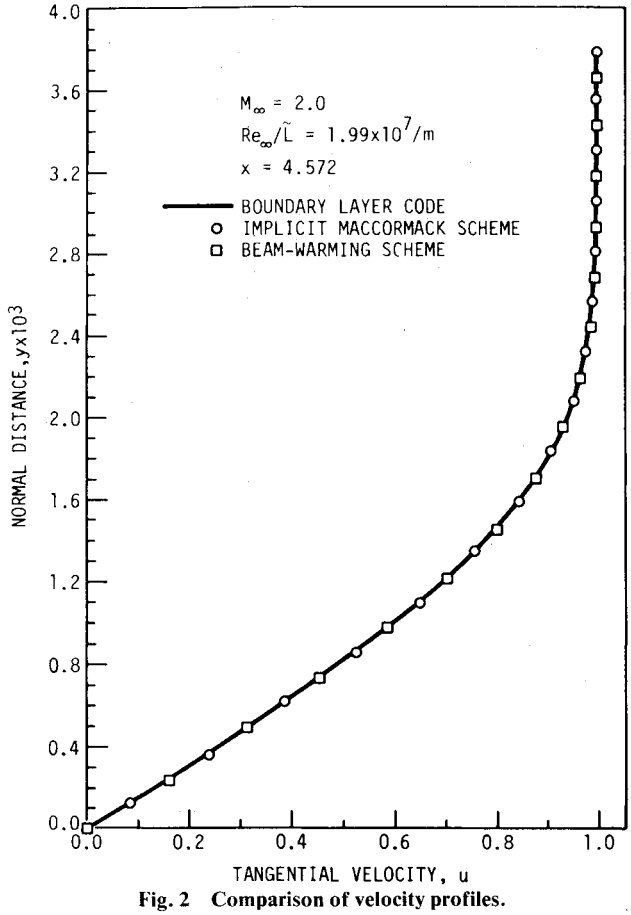

Fig. 2 Comparison of velocity profiles.

dependent variables at the end of each predictor and corrector step.

One of the weaknesses of the present scheme lies in the difficulty of obtaining a reliable implicit boundary condition. That is, at the start of each predictor and corrector sweep, a value for the vector, $(\Delta\xi/\Delta\eta)\,|B|\delta\bar{U}$, is required at the boundary. At boundaries where the flow properties and grid spacing are such that the explicit scheme is stable, this presents no problem since $|B|$ is zero. This is generally the case at freestream boundaries. However, at solid wall boundaries in viscous flow, the grid spacing normal to the wall is generally small and implicit treatment is required. The approach generally taken is that described by MacCormack[6] in which the flux, $|B|\delta\bar{U}$, crossing the boundary at the end of the predictor step is reinjected into the flow to start the corrector sweep. That is,

$$\left[\frac{\Delta\xi}{\Delta\eta}\,|B|\delta\bar{U}\right]_1^{n+1} = [E]\left[\frac{\Delta\xi}{\Delta\eta}\,|B|\delta\bar{U}\right]_2^{n+1} \tag{16}$$

where

$$[E] = \begin{bmatrix} 1 & 0 & 0 & 0 \\ 0 & 1 & 0 & 0 \\ 0 & 0 & -1 & 0 \\ 0 & 0 & 0 & 0 \end{bmatrix}$$

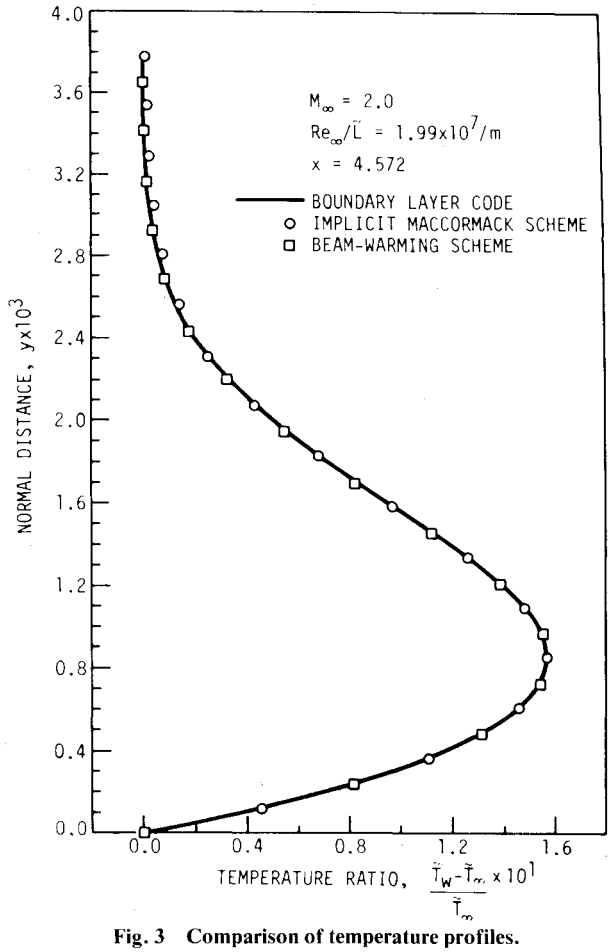

Fig. 3 Comparison of temperature profiles.

Of course, the use of this boundary condition requires that the differencing permutation for the right-hand side of Eqs. (11a) and (12a) remain the same for each step, such that the predictor step is always swept toward the wall and the corrector step away from the wall.

The boundary condition described above was tested on both test cases and its performance was compared with that of the condition which simply sets $[(\Delta\xi/\Delta\eta)\,|B|\delta\bar{U}]_1^{n+1}$ equal to zero. The results will be discussed in the following section.

Numerical Results

In order to evaluate the present implicit method for solving the PNS equations, two test cases were computed.

Test Case 1

For the first test case, the supersonic laminar flow over a flat plate was computed (see Fig. 1). The freestream flow conditions for this case were $M_\infty = 2.0$, $Re_\infty/\tilde{L} = 1.99\times10^7/\text{m}$, $\tilde{T}_\infty = \tilde{T}_w = 233$ K, and $Pr = 0.72$.

Two PNS codes were written to compute this boundary-layer test case. The first code used the conventional Beam-Warming finite difference scheme, while the second employed the implicit MacCormack scheme. The results from the two codes were compared with the results obtained from the compressible boundary-layer code of Pletcher.[16] Thus, a fair evaluation of the suitability of using the implicit MacCormack scheme to solve the PNS equations could be made.

The initial conditions at $x = 1.54$ were obtained from the boundary-layer code. The same equally spaced grid was used in all the calculations with $\Delta y = 6.096\times10^{-5}$. Grid points were added to the top of the mesh as required by the growth of the boundary layer. This followed the procedure of the boundary-layer code and thus allowed a point-by-point comparison of the results.

Profiles of the tangential velocity and temperature at $x = 4.57$ are shown in Figs. 2 and 3, respectively. Figure 4

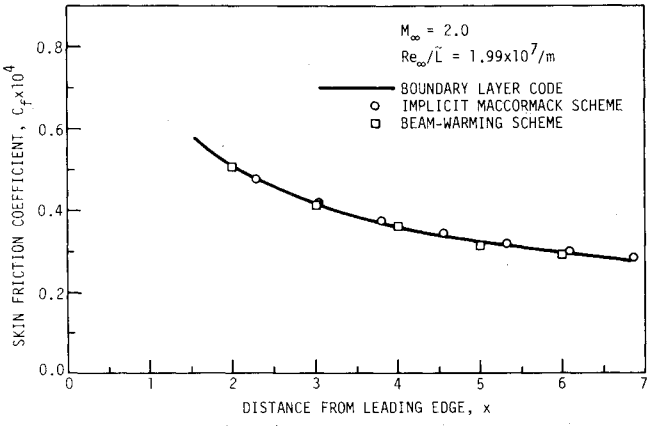

Fig. 4 Comparison of skin-friction coefficients.

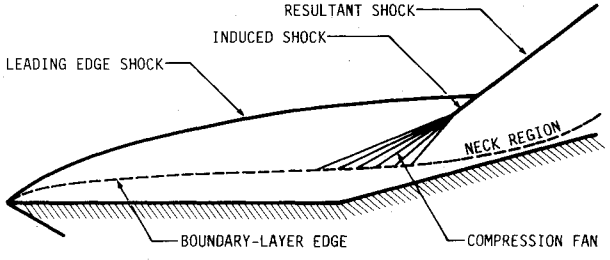

Fig. 5 Hypersonic compression corner test case.

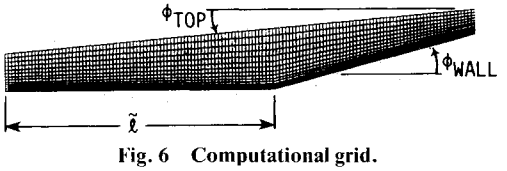

Fig. 6 Computational grid.

shows the streamwise variation of the skin-friction coefficient as calculated from the formula

$$C_f = \frac{\mu_{\text{wall}}}{Re_\infty}\frac{\partial u}{\partial y}$$

Plotted in these three figures are results of the boundary-layer, Beam-Warming PNS, and implicit MacCormack PNS codes. The results are in excellent agreement. Although not shown, calculations were also performed using the explicit MacCormack scheme, which proved to be unstable at a Courant number greater than 1.5. The PNS calculations were performed at a Courant number of 330.

As indicated in the previous section, two different methods of treating the solid boundary were attempted. The first made use of the expression $[\Delta\xi/\Delta\eta\,|B|\delta\bar{U}]_j^{\eta+1}=0$, which caused the scheme to go unstable at Courant numbers larger than approximately 400. The second method consists of reflection of the quantity $\Delta\xi/\Delta\eta\,|B|\delta\bar{U}$ at the wall. This condition allows the new scheme to remain stable at Courant numbers greater than 10^4, although calculated skin-friction coefficients became inaccurate when the Courant number exceeded 5×10^3. The Beam-Warming code, which employs straightforward implicit conditions at both boundaries, was observed to be stable and to yield reasonable results for the skin-friction coefficients at Courant numbers of more than 10^4.

The difference in the accuracy of the two schemes was originally believed to be due to errors introduced by the approximation of the viscous terms on the left-hand side of the implicit MacCormack algorithm. However, a comparison of the results obtained by using the two boundary condition procedures described above indicates the powerful effect of the boundary conditions on the stability and accuracy of the scheme. Observation of this effect leads one to conclude that the boundary condition is likely to still be the dominant source of inaccuracies in implicit MacCormack scheme calculations on equally spaced grids.

Comparison was also made of the computer time required to perform the calculations. Both numerical schemes required about 1.63×10^{-4} s/step/grid point of CPU time on a CRAY-1S computer. It must be pointed out, however, that this is a worst-case value for the implicit MacCormack scheme. That is, since the grid is evenly spaced, all points are calculated implicitly. A timing study was performed to determine the reason why the implicit MacCormack scheme required as much CPU time as the Beam-Warming scheme. As might be expected, a major contributor is the $|B|$ matrix calculation, which must be performed twice per marching step. Another significant factor is the calculation of the right-hand side terms, which also must be computed twice per step. Thus, although the study showed that two block bidiagonal systems can be inverted about 10% more quickly than one block tridiagonal system, some points must be calculated explicitly for the implicit MacCormack scheme to be more efficient in solving the PNS equations than the Beam-Warming scheme.

A comparison of the computer storage requirements of the two schemes showed that the Beam-Warming scheme required 108 Kbytes of storage, while the implicit MacCormack scheme required only 76 Kbytes. The reason for the lower requirements of the implicit MacCormack scheme is that block tridiagonal systems need not be stored for the entire grid. The block bidiagonal systems may be formed and inverted with one sweep while storing only two 4×4 matrices at a time.

The two schemes were of about equal difficulty to code for the two-dimensional PNS equations. The difficulty of coding the viscous Jacobians in the Beam-Warming scheme is balanced by the coding of the $|B|$ matrix in the MacCormack scheme. However, if a code exists that employs the explicit MacCormack scheme, the new scheme may be implemented by simply augmenting the existing algorithm with the implicit steps. The Beam-Warming code of the present study contained about 30% more FORTRAN source lines than the implicit MacCormack scheme, mostly as a result of the block tridiagonal solver.

Test Case II

The second case computed was that of hypersonic laminar flow over a 15 deg wedge. The flow conditions were chosen to correspond with one of the cases studied experimentally by Holden and Moselle[17] and numerically by Hung and MacCormack[15] using the complete Navier-Stokes equations. The flow conditions were

$$M_\infty = 14.1 \qquad \tilde{\ell} = 0.439\ \text{m}$$

$$\tilde{T}_\infty = 72.2\ \text{K} \qquad Pr = 0.72$$

$$Re_\ell = 1.04\times10^5 \qquad \tilde{T}_w = 297\ \text{K}$$

Re_ℓ is the freestream Reynolds number based on the distance from the leading edge to the beginning of the ramp. This flow is supersonic in the inviscid region and exhibits no streamwise separation. Thus, stable space marching is allowed. The problem is illustrated schematically in Fig. 5. The grid used in the calculation is shown in Fig. 6 with every other grid line omitted. Thirty grid points are spaced normal to the wall with a stretching parameter β of 1.08. The grid has an initial height of 0.139 ℓ and the top of the grid is at an angle ϕ_{top} of 5 deg with respect to the horizontal.

The initial conditions at $\bar{x}=0$ were provided by specifying the freestream conditions everywhere except at the wall where

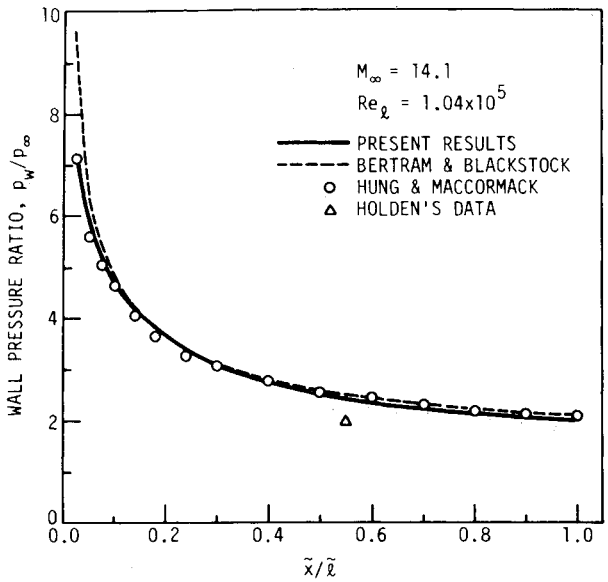

Fig. 7 Wall pressure distribution on the flat plate.

no-slip conditions and constant wall temperature were imposed. The computation then proceeded downstream with a step size of $\Delta\xi = 3.05 \times 10^{-3}$ and was terminated after 266 steps at $\tilde{x} = 1.74\ \tilde{\ell}$. About 1.72 s of CPU time on a CRAY-1S computer were required for the calculation. This compares with the 32 min of computer time on a CDC 7600 that were required by Hung and MacCormack to solve the complete Navier-Stokes equations. It should be noted that about 20 of the 30 points normal to the plate were computed explicitly by the present algorithm.

Comparison of the wall pressures on the flat plate with those computed by Hung and MacCormack is shown in Fig. 7. Also presented in this figure are the theoretical results of the strong interaction analysis of Bertram and Blackstock.[18] Good agreement is observed between the present results and those previously obtained by computational and theoretical methods. A small disagreement with the result of the experiment of Holden and Moselle is observed. The reason for the discrepancy is unknown.

The pressure coefficients defined by $C_p = \tilde{p}_w/\tilde{\rho}_\infty \tilde{V}_\infty^2$ are compared with the previous computational and theoretical results in Fig. 8. Again, the present results compare well with those obtained by other methods. Because of the single-sweep marching, there is slight disagreement in the region near the beginning of the ramp since the flow upstream is not "warned" of the oncoming compression. Nevertheless, the results downstream compare as well with the experiment as those obtained by the complete Navier-Stokes code.

As noted by Hung and MacCormack, the intersection of the leading-edge shock with the shock induced by the wedge results in a type VI interference as classified by Edney.[19] This interference produces an expansion fan that eventually impinges on the wedge surface. However, this point of impingement falls downstream of the region computed in the present calculation and therefore the peak of the computed pressure coefficient is expected to lie downstream of the final ξ station.

Heat-transfer coefficients as calculated from

$$C_H = \frac{\mu_w}{PrRe_\infty} \frac{\sec\theta}{[(\gamma-1)M_\infty^2/2 + 1 - T_w]} \frac{\partial T}{\partial y}$$

are plotted in Fig. 9. The present results show reasonable agreement with the experimental measurements, although some disagreement is observed near the beginning of the ramp.

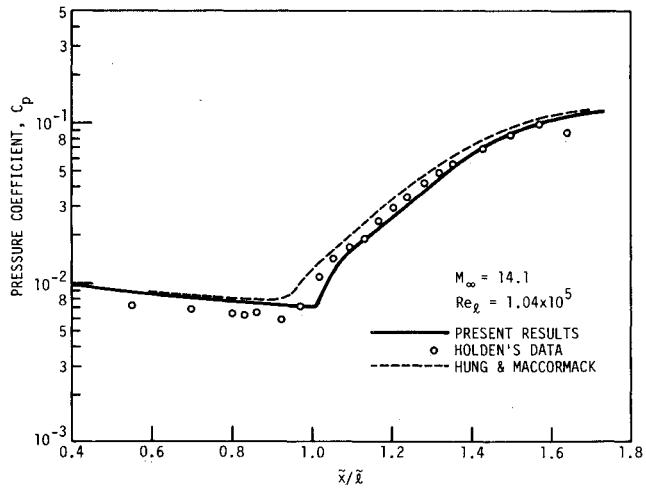

Fig. 8 Comparison of wall pressure coefficients.

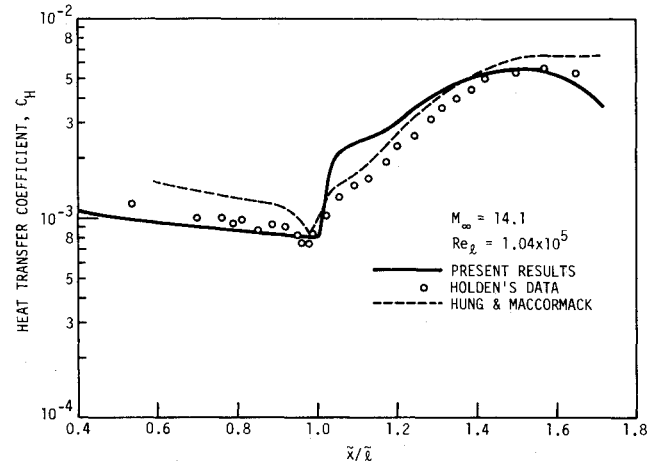

Fig. 9 Comparison of heat-transfer coefficients.

In order to include influences from downstream, and thus hopefully improve the results shown in Figs. 8 and 9, a global iteration on the pressure field of the form suggested by Rakich[14] was incorporated into the PNS code. Calculations of this test case converged in just six iterations. However, the converged results exhibit only a very slight improvement over the previous results.

One source of error in the implicit MacCormack code may be, as in the flat-plate boundary-layer test case, the solid-wall boundary treatment. For that test case, the reflective condition [Eq. (16)] proved to be the more stable and accurate procedure. However, in the present test case, application of Eq. (16) at the wall seemed to trigger instabilities near the beginning of the calculations. For this reason, the quantity $[(\Delta\xi/\Delta\eta)\,|B|\delta\bar{U}]_j^{n+1}$ was set to zero in these computations. Thus, the boundaries are treated explicitly in the implicit MacCormack code, whereas the implicit conditions used in the Beam-Warming code caused no difficulty for this case.

Conclusions

The implicit MacCormack scheme has been applied to the two-dimensional, parabolized Navier-Stokes equations for the computation of steady supersonic viscous flowfields. In order to test this method, two flowfields were computed. These included a laminar flat-plate boundary-layer case and the hypersonic laminar flow over a 15-deg compression corner. The present results compare well with previously published computational results and experimental data.

Appendix: $\partial\bar{E}^*/\partial\bar{U}$, $\partial\bar{F}_i/\partial\bar{U}$, S_y^{-1}, and S_y

The Jacobian $\partial\bar{E}^*/\partial\bar{U}=A$ is given by

$$\frac{\partial\bar{E}^*}{\partial\bar{U}}=\frac{\partial}{\partial\bar{U}}\left(\frac{E^*}{J}\right)=\frac{\partial E^*}{\partial U}$$

and the Jacobian $\partial E^*/\partial U$ is

$$\frac{\partial E^*}{\partial U}=\begin{bmatrix} 0 & 1 & 0 & 0 \\ -u^2+\tfrac{1}{2}\omega(\gamma-1)(u^2+v^2) & [2-(\gamma-1)\omega]u & -\omega(\gamma-1)v & \omega(\gamma-1) \\ -uv & v & u & 0 \\ \left[-\dfrac{\gamma e_t}{\rho}+(\gamma-1)(u^2+v^2)\right]u & \dfrac{\gamma e_t}{\rho}-\dfrac{1}{2}(\gamma-1)(3u^2+v^2) & -(\gamma-1)uv & \gamma u \end{bmatrix}$$

The Jacobian $\partial\bar{F}_i/\partial\bar{U}$, using the fact that $\bar{U}=U/J$, becomes

$$\frac{\partial\bar{F}_i}{\partial\bar{U}}=\eta_x\frac{\partial E}{\partial U}+\eta_y\frac{\partial F}{\partial U}$$

where

$$\frac{\partial E}{\partial U}=\begin{bmatrix} 0 & 1 & 0 & 0 \\ \phi^2-u^2 & (3-\gamma)u & -(\gamma-1)v & \gamma-1 \\ -uv & v & u & 0 \\ \left[-\dfrac{\gamma e_t}{\rho}+2\phi^2\right]u & \dfrac{\gamma e_t}{\rho}-\phi^2-(\gamma-1)u^2 & -(\gamma-1)uv & \gamma u \end{bmatrix}$$

and

$$\frac{\partial F}{\partial U}=\begin{bmatrix} 0 & 0 & 1 & 0 \\ -uv & v & u & 0 \\ \phi^2-v^2 & -(\gamma-1)u & (3-\gamma)v & \gamma-1 \\ \left[-\dfrac{\gamma e_t}{\rho}+2\phi^2\right]v & (\gamma-1)uv & \dfrac{\gamma e_t}{\rho}-\phi^2-(\gamma-1)v^2 & \gamma v \end{bmatrix}$$

where $\phi^2=\tfrac{1}{2}(\gamma-1)(u^2+v^2)$. Defining $V=\eta_x u+\eta_y v$, $\partial\bar{F}_i/\partial\bar{U}$ can be written as

$$\frac{\partial\bar{F}_i}{\partial\bar{U}}=\begin{bmatrix} 0 & \eta_x & \eta_y & 0 \\ \eta_x\phi^2-uV & V+\eta_x(2-\gamma)u & \eta_y u-\eta_x(\gamma-1)v & (\gamma-1)\eta_x \\ \eta_y\phi^2-vV & \eta_x v-\eta_y(\gamma-1)u & V+(2-\gamma)v\eta_y & (\gamma-1)\eta_y \\ \left[-\dfrac{\gamma e_t}{\rho}+2\phi^2\right]V & \eta_x\left(\dfrac{\gamma e_t}{\rho}-\phi^2\right)-(\gamma-1)uV & \eta_y\left(\dfrac{\gamma e_t}{\rho}-\phi^2\right)-(\gamma-1)vV & \gamma V \end{bmatrix}$$

which has eigenvalues

$$\lambda_{1,2}=V,\qquad \lambda_3=V+c\sqrt{\eta_x^2+\eta_y^2},\qquad \lambda_4=V-c\sqrt{\eta_x^2+\eta_y^2}$$

where c is the speed of sound.

Defining

$$\alpha=\frac{\rho}{\sqrt{2}c},\qquad \beta=\frac{1}{\sqrt{2}\rho c},\qquad \hat{\eta}_x=\frac{\eta_x}{\sqrt{\eta_x^2+\eta_y^2}},\qquad \hat{\eta}_y=\frac{\eta_y}{\sqrt{\eta_x^2+\eta_y^2}}\quad\text{and}\quad \hat{V}=\hat{\eta}_x u+\hat{\eta}_y v$$

the matrix of right eigenvectors of $\partial\bar{F}_i/\partial\bar{U}$ is

$$S_y^{-1}=\begin{bmatrix} 1 & 0 & \alpha & \alpha \\ u & \hat{\eta}_y\rho & \alpha(u+\hat{\eta}_x c) & \alpha(u-\hat{\eta}_x c) \\ v & -\hat{\eta}_x\rho & \alpha(v+\hat{\eta}_y c) & \alpha(v-\hat{\eta}_y c) \\ \dfrac{\phi^2}{\gamma-1} & \rho(\hat{\eta}_y u-\hat{\eta}_x v) & \alpha\left(\dfrac{\phi^2+c^2}{\gamma-1}+c\hat{V}\right) & \alpha\left(\dfrac{\phi^2+c^2}{\gamma-1}-c\hat{V}\right) \end{bmatrix}$$

and its inverse is

$$S_y = \begin{bmatrix} 1-\phi^2/c^2 & (\gamma-1)u/c^2 & (\gamma-1)v/c^2 & -(\gamma-1)/c^2 \\ -(\hat{\eta}_y u-\hat{\eta}_x v)/\rho & \hat{\eta}_y/\rho & -\hat{\eta}_x/\rho & 0 \\ \beta(\phi^2-c\hat{V}) & \beta[\hat{\eta}_x c-(\gamma-1)u] & \beta[\hat{\eta}_y c-(\gamma-1)v] & \beta(\gamma-1) \\ \beta(\phi^2+c\hat{V}) & -\beta[\hat{\eta}_x c+(\gamma-1)u] & -\beta[\hat{\eta}_y c+(\gamma-1)v] & \beta(\gamma-1) \end{bmatrix}$$

Acknowledgments

This work was supported by NASA Ames Research Center under Grant NCA2-OR340-301 and the Computational Fluid Dynamics Institute, Iowa State University, Ames, Iowa.

References

[1] Vigneron, Y. C., Rakich, J. V., and Tannehill, J. C., "Calculation of Supersonic Viscous Flow over Delta Wings with Sharp Subsonic Leading Edges," AIAA Paper 78-1137, July 1978.

[2] Schiff, L. B. and Steger, J. L., "Numerical Simulation of Steady Supersonic Viscous Flow," AIAA Paper 79-0130, Jan. 1979.

[3] Lindemuth, I. and Killeen, J., "Alternating Direction Implicit Techniques for Two-Dimensional Magnetohydrodynamics Calculations," *Journal of Computational Physics*, Vol. 13, Oct. 1973, pp. 181-208.

[4] McDonald, H. and Briley, W. R., "Three-Dimesional Supersonic Flow of a Viscous or Inviscid Gas," *Journal of Computational Physics*, Vol. 19, Oct. 1975, pp. 150-178.

[5] Beam, R. and Warming, R. F., "An Implicit Factored Scheme for the Compressible Navier-Stokes Equations," *AIAA Journal*, Vol. 16, April 1978, pp. 393-401.

[6] MacCormack, R. W., "A Numerical Method for Solving the Equations of Compressible Viscous Flow," AIAA Paper 81-0110, Jan. 1981.

[7] MacCormack, R.W., "The Effect of Viscosity on Hypervelocity Impact Cratering," AIAA Paper 69-354, April 1969.

[8] von Lavante, E. and Thompkins, W.T., "An Implicit Bidiagonal Numerical Method for Solving the Navier-Stokes Equations," AIAA Paper 82-63, Jan. 1982.

[9] Kumar, A., "Some Observations on a New Numerical Method for Solving the Navier-Stokes Equations," NASA TP-1934, 1981.

[10] Kordulla, W. and MacCormack, R. W., "Transonic Flow Computation Using an Explicit-Implicit Method," *Proceedings of the Eighth International Conference on Numerical Methods*, Springer-Verlag, Aachen, FRG, June-July 1982, pp. 286-295.

[11] Gupta, R. N., Gnoffo, P. A., and MacCormack, R. W., "A Viscous Shock-Layer Flowfield Analysis by an Explicit-Implicit Method," AIAA Paper 83-1423, June 1983.

[12] White, M. E. and Anderson, J. D. Jr., "Application of MacCormack's Implicit Method to Quasi-One-Dimensional Nozzle Flows," AIAA Paper 82-0992, June 1982.

[13] Shang, J. S. and MacCormack, R. W., "Flow Over a Biconic Configuration with an Afterbody Compression Flap—A Comparative Numerical Study," AIAA Paper 83-1668, July 1983.

[14] Rakich, J. V., "Iterative PNS Method for Attached Flows with Upstream Influence," AIAA Paper 83-1955, July 1983.

[15] Hung, C. M. and MacCormack, R. W., "Numerical Solutions of Supersonic and Hypersonic Laminar Compression Corner Flows," *AIAA Journal*, Vol. 14, April 1976, pp. 475-481.

[16] Pletcher, R. H., "On a Calculation Method for Compressible Turbulent Boundary Layer Flows with Heat Transfer," AIAA Paper 71-165, Jan. 1971.

[17] Holden, M. S. and Moselle, J. R., "Theoretical and Experimental Studies of the Shock Wave-Boundary Layer Interaction on Compression Surfaces in Hypersonic Flow," CALSPAN, Buffalo, N.Y., Rept. AF-2410-A-1, Oct. 1969.

[18] Bertram, M. H. and Blackstock, T. A., "Some Simple Solutions to the Problem of Predicting Boundary-Layer Self-Induced Pressure," NASA TN D-798, April 1961.

[19] Edney, B., "Anomalous Heat-Transfer and Pressure Distributions on Blunt Bodies at Hypersonic Speeds in the Presence of an Impinging Shock," Aeronautical Research Institute of Sweden, Stockholm, FFA Rept. 116, 1968.